



# Hybrid control strategy of delayed neural networks and its application to sampled-data systems: an impulsive-based bilateral looped-functional approach

Shiyu Dong · Hong Zhu · Shouming Zhong ·  
Kaibo Shi · Yong Zeng

Received: 27 April 2021 / Accepted: 23 July 2021 / Published online: 7 August 2021  
© The Author(s), under exclusive licence to Springer Nature B.V. 2021

**Abstract** In this work, the problem of hybrid control strategy for delayed neural networks is investigated via an impulsive-based bilateral looped-functional (IBBLF) approach. Firstly, a hybrid controller is introduced, which includes feedback control and impulsive control, and the feedback control plays a vital role in the case of impulsive perturbation. Secondly, an IBBLF is constructed to relax the requirement of positive definiteness and only satisfies it at the impulsive instants, which reduces the conservatism of the stability results. Thirdly, the construction of IBBLF takes full advantage of the state information on both the intervals  $z(t_k^+)$  to  $z(t)$  and  $z(t)$  to  $z(t_{k+1})$ , then combining with a proposed lemma, exponential stability criteria with less conservative are obtained. In addition, the obtained

results are applied to nonlinear sampled-data systems. Finally, two numerical examples are presented to certify the effectiveness and superiority of the theoretical results.

**Keywords** Hybrid control · Impulsive-based bilateral looped functional · Delayed neural networks · Impulsive effects

## 1 Introduction

With the heuristics of the biological nervous system, neural networks (NNs) have been proven to be the key to solving various difficult problems in many fields [1–5]. The response of the NNs to the weak envelope modulation signal formed by the superposition of two periodic signals with different frequencies was studied in [6]. Artificial NNs, as a method of local search heuristics, [7] proposed differential evolutionary hybridization algorithms to predict the optimal strategy or to generate better offspring from a set of differential evolutionary strategies. In order to improve the classification accuracy of diabetes diagnosis, [8] used Watts-Strogatz small-world feedforward NNs (SWFNNs) and Newman-Watts SWFNNs for analysis, and proved that Newman-Watts SWFNNs analysis method can obtain the best output error parameters and the highest output correlation.

In practical engineering, the communication time and the switching speed of the amplifiers may be

---

S. Dong (✉) · H. Zhu · Y. Zeng  
School of Automation Engineering, University of  
Electronic Science and Technology of China, Chengdu  
611731, China  
e-mail: dsy\_shiyu@163.com

H. Zhu  
e-mail: zhuhong@uestc.edu.cn

Y. Zeng  
e-mail: zengyong99@uestc.edu.cn

S. Zhong  
School of Mathematical Sciences, University of Electronic  
Science and Technology of China, Chengdu 611731, China  
e-mail: zhongsm@uestc.edu.cn

K. Shi  
School of Electronic Information and Electrical  
Engineering, Chengdu University, Chengdu 610106, China  
e-mail: skbs111@163.com

limited between neurons. Since the existence of time delays is frequently a source of instability, weak performance [9–11]. And the stability of the system is one of the prerequisites to study the performance of the system. Therefore, the stability analysis of DNNs is important theoretical significance and practical value [12–14].

In the natural and artificial world, only a few networks can adjust their system parameters to achieve stability. In order to overcome this problem, most networks need to rely on some external force, that is, controllers [15]. Thus, various control methods have been introduced to stabilize the DNNs, such as intermittent control [16], sliding mode control [17, 18], state feedback control [19, 20], event-triggered control [21], impulsive control [22–25], sampled-data control [26–29]. Among these commonly used control methods, discontinuous control (including impulsive control and intermittent control), are more effective than other control methods in terms of reducing control costs. The control mechanism of these two discontinuous control methods is: intermittent control is activated within a certain time interval, that is, intermittent control controls the state of the system within a specific interval, while impulsive control is only activated at discrete instants.

Obviously, the impulsive control mechanism is less cost than intermittent control mechanism [30]. In addition, for many real networks, the state of nodes is often disturbed instantaneously, and there will be sudden changes at some instants. These sudden changes may be produced by sudden noises, frequency changes or other switching phenomena. In other words, there exists impulsive effects [31, 32]. Therefore, impulsive control is the most consistent with the actual situation and more effective in reducing the control cost. Generally, in the dynamic analysis of the DNNs, there are two types of impulses: stable impulses and unstable impulses. If the impulsive effects can destroy the stability of DNNs, then the impulse sequence is called unstable impulse. Meanwhile, if the corresponding impulsive effects can promote the stability of DNNs, the impulse sequence is called stable impulse. What's more, when the impulsive effects are unstable impulse, the impulse should not occur too frequently in order to achieve the goal of stability. Similarly, when the impulsive effects are stable impulse, the impulsive interval should not be too long, otherwise it will affect the stability of the DNNs. To solve this difficulty, many literatures used

the upper and lower bounds of the impulsive interval to control the frequency of impulses occurring [33–37]. In [22], authors proposed a unified criterion to investigate the synchronization of impulsive dynamical networks. Unfortunately, using the upper or lower bounds to characterize the impulses frequency may lead to conservative results. Thus, in order to get less conservative results, what can we do to obtain more relax results for the occurrence of the impulse and not even impose any restrictions on the impulse? and it works for both stable impulses and unstable impulses.

In most studies, the traditional Lyapunov functional is used to obtain the stability/synchronization of the impulsive systems. However, the drawback of the classical Lyapunov theory is that the constructed functional must satisfy the positive definiteness characterization in the whole impulsive interval, which will cause the result to be quite conservative. Thus, a looped-functional method (LFM) was developed [38] in order to get a less conservative result. It's shown that the LFM satisfies the positive definiteness at the sampling instants, which not only reduces the conservatism, but also obtains a larger sampling interval. Then on this basis, many studies used the LFM to study the asymptotic stability of the SDSs [39, 40]. In [41–44], LFM was applied to the impulsive systems, but these papers have the following shortcomings: (1) The systems they studied were linear impulse systems, and only studied the asymptotic stability of system. (2) Due to the constructed one-sided looped-functional, the information of the impulsive instant was not fully utilized, resulting in a certain conservatism. Hence, the stability problem of impulsive DNNs based on bilateral looped-functional has not been fully investigated, and it is still an open and challenging problem.

Motivated by the above analysis, the positive effects and negative effects of impulses for DNNs are analyzed in this work. When the impulse has a negative effect for DNNs, the linear feedback control in the hybrid controller can be used to balance the negative effect, and then the system stability can be obtained by using the IBBLF method. On the contrary, if the impulse plays a positive role in the stability of the DNNs, then only the impulsive controller can achieve the expected results under IBBLF.

The main highlights of this work are shown as follows:

**Table 1** Notations

Notation	Definition
$\mathbb{N}^+$	The set of positive integers
$\mathcal{R}$	The set of real numbers
$\mathcal{R}^+$	The non-negative real numbers
$\mathcal{R}^n$	The Euclidean space of $n$ -dimensional
$\mathcal{R}^{m \times n}$	The set of $m \times n$ real matrices
$\mathcal{Q}^T$	The transpose of any square matrix $\mathcal{Q}$
$\mathcal{Q}^{-1}$	The inverse of any square matrix $\mathcal{Q}$
$\text{He}\{\mathcal{Q}\}$	The sum of $\mathcal{Q}$ and $\mathcal{Q}^T$ ( $\mathcal{Q} + \mathcal{Q}^T$ )
$\text{diag}\{\dots\}$	The diagonal matrix
$\text{col}\{\dots\}$	The column vector
$I$	An identity matrix of suitable dimension
$\ \cdot\ $	The induced matrix norm
$\star$	A symmetric block in any symmetric matrix
$\lambda_{\max}(\mathcal{Q})$	The maximum eigenvalue of matrix $\mathcal{Q}$
$\lambda_{\min}(\mathcal{Q})$	The minimum eigenvalue of matrix $\mathcal{Q}$
$\mathbb{K}$	The set of differentiable functions defined, as an interval $[0, T]$ to $\mathcal{R}^n$ , where $T \in \mathcal{R}^+$

- (1) In order to consider both stable and unstable impulses at the same time, a hybrid controller is developed, in which the feedback controller is used to coordinate the impulsive controller.
- (2) An improved IBBLF is constructed, which relaxes the requirement of positive definiteness. In addition, the functional introduces the cross-terms of the state and the integral of impulsive instants and takes the information on both impulsive instants  $z(t_k^+)$  and  $z(t_{k+1})$  into account.
- (3) A novel lemma is presented by using Cauchy-Schwarz inequality and Gronwall-Bellman inequality. Furthermore, discrete-time exponential stability conditions are derived based on the constructed IBBLF method, and less conservative exponential stability criteria are obtained in the light of linear matrix inequalities (LMIs).
- (4) The exponential stability results of impulsive systems are applied to SDSs with variable sampling and time-varying delay, and compared with the Refs. [28, 45, 46], one can obtain a larger allowable upper bound.

## 2 Preliminaries and problem statement

The following DNNs with external input are considered:

$$\begin{cases} \dot{z}(t) = \mathcal{A}z(t) + \mathcal{B}g(z(t)) + \mathcal{C}h(z(t - \tau(t))) + u(t), \\ z(s) = \varphi(s), \quad s \in [-\tau, 0], \end{cases} \tag{1}$$

where the state vector  $z(t) = \text{col}\{z_1(t), z_2(t), \dots, z_n(t)\} \in \mathcal{R}^n$ ,  $0 \leq \tau(t) \leq \tau$  denotes the time-varying delay and satisfies  $\dot{\tau}(t) \leq \mu \leq 1$ ,  $g(z(t)) = \text{col}\{g_1(z_1(t)), g_2(z_2(t)), \dots, g_n(z_n(t))\} \in \mathcal{R}^n$  and  $h(z(t - \tau(t))) = \text{col}\{h_1(z_1(t - \tau(t))), h_2(z_2(t - \tau(t))), \dots, h_n(z_n(t - \tau(t)))\} \in \mathcal{R}^n$  are the activation functions and satisfy  $g_i(0) = h_i(0) = 0$ .  $\mathcal{A} = \text{diag}\{a_1, a_2, \dots, a_n\} \in \mathcal{R}^{n \times n}$  denotes the self-inhibition matrix, where  $a_i < 0$  ( $i = 1, 2, \dots, n$ ),  $\mathcal{B}, \mathcal{C} \in \mathcal{R}^{n \times n}$  represent the connection weight of the activation functions  $g(\cdot), h(\cdot), u(t) \in \mathcal{R}^n$  is the control input to be designed.

**Assumption 1** [47]. The  $g_i(\cdot), h_i(\cdot)$  are Lipschitz's continuous activation functions, and there are constants  $\mathcal{G}_i > 0, \mathcal{H}_i > 0$ , such that

$$\begin{aligned} 0 &\leq \frac{g_i(\mu_1) - g_i(\mu_2)}{\mu_1 - \mu_2} \leq \mathcal{G}_i, \\ 0 &\leq \frac{h_i(\mu_1) - h_i(\mu_2)}{\mu_1 - \mu_2} \leq \mathcal{H}_i, \end{aligned}$$

where  $i = 1, 2, \dots, n, \mu_1 \neq \mu_2$ .

For system (1), the following hybrid control strategy is considered:

$$\begin{aligned} u(t) &= u_1(t) + u_2(t), \\ u_1(t) &= -\Gamma z(t), \quad u_2(t) = \sum_{k=1}^{\infty} \mathcal{Q}z(t)\delta(t - t_k), \end{aligned} \tag{2}$$

where  $\Gamma = \text{diag}\{\gamma_1, \gamma_2, \dots, \gamma_n\} \geq 0$  is the feedback gain,  $\mathcal{Q}$  means the strength of impulse,  $\delta(\cdot)$  is the Dirac function and  $\{t_k\}_{k=1}^{\infty}, \lim_{k \rightarrow \infty} t_k = \infty$  is the impulsive sequence. The impulsive interval is defined as  $\mathcal{T}_k = t_{k+1} - t_k \in [\mathcal{T}_m, \mathcal{T}_M]$ .  $z(t)$  is supposed to be left-continuous (that is:  $z(t_k) = z(t_k^-)$ ) and has right-limits.

Substituting (2) into (1), one has

$$\begin{cases} \dot{z}(t) = (\mathcal{A} - \Gamma)z(t) + \mathcal{B}g(z(t)) + \mathcal{C}h(z(t - \tau(t))), & t \neq t_k, \\ \Delta z(t_k) = \mathcal{Q}z(t_k), & t = t_k, \quad k \in \mathbb{N}^+, \\ z(s) = \varphi(s), & s \in [-\tau, 0], \end{cases} \tag{3}$$

where  $\Delta z(t_k) = z(t_k^+) - z(t_k^-)$ . Next, some effective lemmas and definition are introduced.

**Definition 1** [41]. The functional  $f$  satisfies the following mapping

$$f : [0, \mathcal{T}_M] \times \mathbb{K}_{[\mathcal{T}_m, \mathcal{T}_M]} \times [\mathcal{T}_m, \mathcal{T}_M] \rightarrow \mathcal{R},$$

where  $0 < \epsilon \leq \mathcal{T}_m \leq \mathcal{T}_M < +\infty$ . If the following conditions are satisfied, then the functional  $f$  is called looped-functional.

- 1.  $f$  satisfies the characteristics of periodic

$$f(0, x, \mathcal{T}_k) = f(\mathcal{T}_k, x, \mathcal{T}_k), \tag{4}$$

for  $\forall x \in C([0, \mathcal{T}_k], \mathcal{R}^n) \subset \mathbb{K}_{[\mathcal{T}_m, \mathcal{T}_M]}$ ,  $\mathcal{T}_k \in [\mathcal{T}_m, \mathcal{T}_M]$ .

- 2. It's differentiable with respect to the first variable.

**Lemma 1** [48]. Constants  $T > 0$ ,  $c \geq 0$ ,  $r \geq 0$ . Let  $u(t)$  be a Borel measurement bounded nonnegative function on  $[t_0, T]$ , and  $g(t)$  be a nonnegative integral function on  $[t_0, T]$ . If

$$u(t) \leq c + \int_{t_0}^t [g(s)u(s) + r]ds, \quad \text{for } \forall t_0 \leq t \leq T,$$

then

$$u(t) \leq [c + r(t - t_0)] \exp \left( \int_{t_0}^t g(s)ds \right).$$

**Lemma 2** For system (3), the following inequality holds for  $t \in (t_k^+, t_{k+1}]$ :

$$\|z(t)\|^2 \leq \theta_1 \|z(t_k)\|^2 + \theta_2 \int_{t_k - \tau(t_k)}^{t_k} \|z(s)\|^2 ds, \tag{5}$$

where

$$\begin{aligned} \mathcal{G} &= \text{diag}\{\mathcal{G}_1, \mathcal{G}_2, \dots, \mathcal{G}_n\}, \\ \mathcal{H} &= \text{diag}\{\mathcal{H}_1, \mathcal{H}_2, \dots, \mathcal{H}_n\}, \\ \theta_1 &= 4e^\sigma \|I + \mathcal{Q}\|^2, \end{aligned}$$

$$\begin{aligned} \theta_2 &= \frac{4}{1 - \mu} e^\sigma \mathcal{T}_M \|C\|^2 \|\mathcal{H}\|^2, \\ \sigma &= 4\mathcal{T}_M^2 (\|\mathcal{A} - \Gamma\|^2 + \|\mathcal{B}\|^2 \|\mathcal{G}\|^2 \\ &\quad + \frac{\|C\|^2 \|\mathcal{H}\|^2}{1 - \mu}). \end{aligned}$$

*Proof* From system (3), we can obtain

$$\begin{aligned} z(t) &= z(t_k^+) + \int_{t_k}^t (\mathcal{A} - \Gamma)z(s)ds \\ &\quad + \int_{t_k}^t \mathcal{B}g(z(s))ds \\ &\quad + \int_{t_k}^t \mathcal{C}h(z(s - \tau(s)))ds. \end{aligned} \tag{6}$$

According to inequalities  $\|\mathcal{B}g(z(t))\|^2 \leq \|\mathcal{B}\|^2 \|\mathcal{G}\|^2 \|z(t)\|^2$ ,  $\|\mathcal{C}h(z(t - \tau(t)))\|^2 \leq \|C\|^2 \|\mathcal{H}\|^2 \|z(t - \tau(t))\|^2$ , and by using Cauchy-Schwarz inequality, one can derive

$$\begin{aligned} \|z(t)\|^2 &\leq 4\|z(t_k^+)\|^2 + 4 \left\| \int_{t_k}^t (\mathcal{A} - \Gamma)z(s)ds \right\|^2 \\ &\quad + 4 \left\| \int_{t_k}^t \mathcal{B}g(z(s))ds \right\|^2 + 4 \left\| \int_{t_k}^t \mathcal{C}h(z(s - \tau(s)))ds \right\|^2 \\ &\leq 4\|I + \mathcal{Q}\|^2 \|z(t_k)\|^2 + 4\mathcal{T}_M \|\mathcal{A} - \Gamma\|^2 \int_{t_k}^t \|z(s)\|^2 ds \\ &\quad + 4\mathcal{T}_M \|\mathcal{B}\|^2 \|\mathcal{G}\|^2 \int_{t_k}^t \|z(s)\|^2 ds + 4\mathcal{T}_M \|C\|^2 \|\mathcal{H}\|^2 \\ &\quad \times \int_{t_k - \tau(t_k)}^t \|z(s)\|^2 ds \\ &= 4\|I + \mathcal{Q}\|^2 \|z(t_k)\|^2 + 4\mathcal{T}_M \left( \|\mathcal{A} - \Gamma\|^2 + \|\mathcal{B}\|^2 \|\mathcal{G}\|^2 \right. \\ &\quad \left. + \frac{\|C\|^2 \|\mathcal{H}\|^2}{1 - \mu} \right) \int_{t_k}^t \|z(s)\|^2 ds + \frac{4\mathcal{T}_M \|C\|^2 \|\mathcal{H}\|^2}{1 - \mu} \\ &\quad \times \int_{t_k - \tau(t_k)}^{t_k} \|z(s)\|^2 ds. \end{aligned} \tag{7}$$

Then, for  $t \in (t_k^+, t_{k+1}]$ , applying Lemma 1, one has

$$\|z(t)\|^2 \leq \theta_1 \|z(t_k)\|^2 + \theta_2 \int_{t_k - \tau(t_k)}^{t_k} \|z(s)\|^2 ds. \tag{8}$$

### 3 Main results

#### 3.1 The analysis of exponential stability based on an IBBLF approach

For convenience, one will use the following notations in Theorem 1.

$$\begin{aligned} \pi_1(t) &= \frac{1}{t-t_k} \int_{t_k}^t z(s)ds, \\ \pi_2(t) &= \frac{1}{t_{k+1}-t} \int_t^{t_{k+1}} z(s)ds, \\ \eta_1(t) &= \text{col}\{z(t_k^+), z(t_{k+1})\}, \\ \eta_2(t) &= \text{col}\{z(t) - z(t_k^+), z(t) - z(t_{k+1})\}, \\ \eta_3(t) &= \text{col}\{(t_{k+1}-t)(z(t)-z(t_k^+)), (t-t_k)(z(t)-z(t_{k+1}))\}, \\ \eta_4(t) &= \text{col}\{z(t), z(t_k), z(t_{k+1})\}, \\ \eta_5(t) &= \text{col}\{\pi_1(t), \pi_2(t), g(z(t)), h(z(t-\tau(t)))\}, \\ \xi(t) &= \text{col}\{z(t), z(t-\tau(t)), z(t_k), z(t_{k+1}), \dot{z}(t), \eta_5(t)\}, \\ e_j &= [0_{n \times (j-1)n}, I_{n \times n}, 0_{n \times (j-1)n}], \quad j = 1, 2, \dots, 9. \end{aligned}$$

**Theorem 1** *Given constants  $\mathcal{T}_m > 0, \mathcal{T}_M > 0, \alpha > 0$ , the system (3) is exponential stable if there exist matrices  $P_j > 0, X_j > 0, M_1 > 0, N_1 > 0$ , diagonal matrices  $\Lambda_j > 0$ , symmetric matrix  $S$  and arbitrary appropriate dimensions matrices  $Q_j, R, L_j, \mathcal{D}_j, Y, Z, M_\kappa, N_\kappa, j = 1, 2, \iota = 1, 2, 3, \kappa = 2, 3$ , such that the following LMIs hold:*

$$\begin{bmatrix} P_1 (I + \mathcal{D})P_1 \\ \star & P_1 \end{bmatrix} > 0, \tag{9}$$

$$\mathcal{L}_1 = \begin{bmatrix} X_1 & L_1 \\ \star & X_2 \end{bmatrix} > 0, \tag{10}$$

$$\mathcal{L}_2 = \begin{bmatrix} 3X_1 & L_2 \\ \star & 3X_2 \end{bmatrix} > 0, \tag{11}$$

$$\Omega_1(\mathcal{T}_k) = \Xi_1 + \mathcal{T}_k \Xi_2 < 0, \tag{12}$$

$$\Omega_2(\mathcal{T}_k) = \Xi_1 + \mathcal{T}_k \Xi_3 < 0, \tag{13}$$

where  $\Xi_1, \Xi_2$  and  $\Xi_3$  are defined in Appendix A.

*Proof* Construct the following time-dependent IBBLF:

$$\mathcal{W}(t) = \mathcal{V}_1(t) + \mathcal{V}_2(t), \quad t \in (t_k^+, t_{k+1}], \tag{14}$$

where  $\mathcal{V}_1(t) = V_1(t) + V_2(t), \mathcal{V}_2(t) = \sum_{i=3}^7 V_i(t)$  and

$$V_1(t)d = z^T(t)P_1z(t),$$

$$V_2(t) = \int_{t-\tau(t)}^t e^{2\alpha(s-t)} z^T(s)P_2z(s)ds,$$

$$V_3(t) = 2\eta_3^T(t)[Q_1\eta_1(t) + Q_2\eta_2(t)],$$

$$V_4(t) = 2[z(t) - z(t_k^+)]^T R[z(t) - z(t_{k+1})],$$

$$V_5(t) = (t_{k+1} - t)(t - t_k)\eta_1^T(t)S\eta_1(t),$$

$$\begin{aligned} V_6(t) &= (t_{k+1} - t)(t_{k+1} - t_k) \int_{t_k}^t e^{2\alpha(s-t)} \dot{z}^T(s)X_1\dot{z}(s)ds \\ &\quad - (t - t_k)(t_{k+1} - t_k) \int_t^{t_{k+1}} e^{2\alpha(s-t)} \dot{z}^T(s)X_2\dot{z}(s)ds, \end{aligned}$$

$$\begin{aligned} V_7(t) &= (t_{k+1} - t) \int_{t_k}^t e^{2\alpha(s-t)} \eta_4^T(s)\mathcal{M}\eta_4(s)ds \\ &\quad - (t - t_k) \int_t^{t_{k+1}} e^{2\alpha(s-t)} \eta_4^T(s)\mathcal{N}\eta_4(s)ds, \end{aligned}$$

with

$$\begin{aligned} Q_1 &= \begin{bmatrix} Q_{11} & Q_{12} \\ Q_{13} & Q_{14} \end{bmatrix}, \quad Q_2 = \begin{bmatrix} Q_{21} & Q_{22} \\ Q_{23} & Q_{24} \end{bmatrix}, \quad S = \begin{bmatrix} S_{11} & S_{12} \\ \star & S_{22} \end{bmatrix}, \\ \mathcal{M} &= \begin{bmatrix} M_1 & Y_1 & Y_2 \\ \star & M_2 & Y_3 \\ \star & \star & M_3 \end{bmatrix}, \quad \mathcal{N} = \begin{bmatrix} N_1 & Z_1 & Z_2 \\ \star & N_2 & Z_3 \\ \star & \star & N_3 \end{bmatrix}. \end{aligned}$$

Taking the derivative of  $\mathcal{W}(t)$ , one obtains

$$\begin{aligned} \dot{V}_1(t) + 2\alpha V_1(t) &= \xi^T(t)He\{e_1^T P_1 e_5 + \alpha e_1^T P_1 e_1\}\xi(t), \tag{15} \end{aligned}$$

$$\begin{aligned} \dot{V}_2(t) + 2\alpha V_2(t) &\leq \xi^T(t)\{e_1^T P_2 e_1 - (1 - \mu)e^{-2\alpha\tau} e_2^T P_2 e_2\}\xi(t), \tag{16} \end{aligned}$$

$$\begin{aligned} \dot{V}_3(t) + 2\alpha V_3(t) &= \xi^T(t)He\{\Sigma_6^T Q_1 \Sigma_1 + \Sigma_6^T Q_2 \Sigma_2 + (t - t_k)(\Sigma_8^T \\ &\quad \times Q_1 \Sigma_1 + \Sigma_8^T Q_2 \Sigma_2 + \Sigma_5^T Q_2 \Sigma_3 + 2\alpha \Sigma_5^T Q_1 \Sigma_1 \\ &\quad + 2\alpha \Sigma_5^T Q_2 \Sigma_2) + (t_{k+1} - t)(\Sigma_7^T Q_1 \Sigma_1 + \Sigma_7^T Q_2 \Sigma_2 \\ &\quad + \Sigma_4^T Q_2 \Sigma_3 + 2\alpha \Sigma_4^T Q_1 \Sigma_1 + 2\alpha \Sigma_4^T Q_2 \Sigma_2)\}\xi(t), \tag{17} \end{aligned}$$

$$\begin{aligned} \dot{V}_4(t) + 2\alpha V_4(t) &= \xi^T(t)He\{e_5^T R(e_1 - e_4) + (e_1 - (I + \mathcal{D})e_3)^T \\ &\quad \times Re_5 + 2\alpha(e_1 - (I + \mathcal{D})e_3)^T R(e_1 - e_4)\}\xi(t), \tag{18} \end{aligned}$$

$$\begin{aligned} \dot{V}_5(t) + 2\alpha V_5(t) &= \xi^T(t)\{(t_{k+1} - t)\Sigma_1^T S \Sigma_1 - (t - t_k)\Sigma_1^T S \Sigma_1 \\ &\quad + 2\alpha(t_{k+1} - t)(t - t_k)\Sigma_1^T S \Sigma_1\}\xi(t), \tag{19} \end{aligned}$$

$$\dot{V}_6(t) + 2\alpha V_6(t)$$

$$\begin{aligned} &\leq \xi^T(t) \{ (t_{k+1} - t) \mathcal{T}_k e_5^T X_1 e_5 \} \xi(t) - \mathcal{T}_k \int_{t_k}^t e^{-2\alpha \mathcal{T}_M} \\ &\times \dot{z}^T(s) X_1 \dot{z}(s) ds + \xi^T(t) \{ (t - t_k) \mathcal{T}_k e_5^T X_2 e_5 \} \\ &\times \xi(t) - \mathcal{T}_k \int_t^{t_{k+1}} \dot{z}^T(s) X_2 \dot{z}(s) ds, \end{aligned} \tag{20}$$

$$\begin{aligned} &\dot{V}_7(t) + 2\alpha V_7(t) \\ &\leq -e^{-2\alpha \mathcal{T}_M} \int_{t_k}^t z^T(s) M_1 z(s) ds + (t - t_k) \xi^T(t) \Phi_1 \xi(t) \\ &+ (t_{k+1} - t) \xi^T(t) \Phi_2 \xi(t) - \int_t^{t_{k+1}} z^T(s) N_1 z(s) ds \\ &+ (t - t_k) \xi^T(t) \Phi_3 \xi(t) + (t_{k+1} - t) \xi^T(t) \Phi_4 \xi(t). \end{aligned} \tag{21}$$

For the integral terms of (20) and (21), one has

$$\begin{aligned} &-\mathcal{T}_k \int_{t_k}^t e^{-2\alpha \mathcal{T}_M} \dot{z}^T(s) X_1 \dot{z}(s) ds - \mathcal{T}_k \int_t^{t_{k+1}} \dot{z}^T(s) X_2 \dot{z}(s) ds \\ &\leq \xi^T(t) \{ -\Phi_5^T \mathcal{L}_1 \Phi_5 - \Phi_6^T \mathcal{L}_2 \Phi_6 \} \xi(t), \tag{22} \\ &-e^{-2\alpha \mathcal{T}_M} \int_{t_k}^t z^T(s) M_1 z(s) ds - \int_t^{t_{k+1}} z^T(s) N_1 z(s) ds \\ &\leq \xi^T(t) \{ -(t - t_k) e^{-2\alpha \mathcal{T}_M} e_6^T M_1 e_6 - (t_{k+1} - t) \\ &\times e_7^T N_1 e_7 \} \xi(t). \end{aligned} \tag{23}$$

Therefore, one obtains

$$\begin{aligned} &\dot{V}_6(t) + 2\alpha V_6(t) \\ &\leq \xi^T(t) \{ (t_{k+1} - t) \mathcal{T}_M e_5^T X_1 e_5 + (t - t_k) \mathcal{T}_M e_5^T X_2 e_5 \\ &- \Phi_5^T \mathcal{L} \Phi_5 - \Phi_6^T \mathcal{L}_2 \Phi_6 \} \xi(t), \tag{24} \\ &\dot{V}_7(t) + 2\alpha V_7(t) \\ &\leq \xi^T(t) \{ (t - t_k) (\Phi_1 + \Phi_3 - e^{2\alpha \mathcal{T}_M} e_6^T M_1 e_6) \\ &+ (t_{k+1} - t) (\Phi_2 + \Phi_4 - e_7^T N_1 e_7) \} \xi(t). \end{aligned} \tag{25}$$

In addition, for any diagonal matrices  $\Lambda_1 > 0, \Lambda_2 > 0$ , the following inequalities hold:

$$\begin{aligned} &\xi^T(t) \text{He} \{ e_8^T \Lambda_1 (\mathcal{G} e_1 - e_8) \} \xi(t) \geq 0, \\ &\xi^T(t) \text{He} \{ e_9^T \Lambda_2 (\mathcal{H} e_2 - e_9) \} \xi(t) \geq 0. \end{aligned} \tag{26}$$

For any matrices  $\mathcal{D}_1 \in \mathcal{R}^{n \times n}, \mathcal{D}_2 \in \mathcal{R}^{n \times n}$ , one can get:

$$\xi^T(t) H e \{ \Phi_7^T \Phi_8 \} \xi(t) = 0. \tag{27}$$

From (15–28), the estimation of  $\dot{\mathcal{W}}(t) + 2\alpha \mathcal{W}(t)$  will be obtained:

$$\begin{aligned} &\dot{\mathcal{W}}(t) + 2\alpha \mathcal{W}(t) \\ &w_1 q \leq \xi^T(t) \{ \Xi_1 + (t - t_k) \Xi_2 + (t_{k+1} - t) \Xi_3 \} \xi(t). \end{aligned} \tag{28}$$

Then, one obtains

$$\begin{aligned} &\dot{\mathcal{W}}(t) + 2\alpha \mathcal{W}(t) \\ &\leq \xi^T(t) \left\{ \frac{t - t_k}{\mathcal{T}_k} \Omega_1(\mathcal{T}_k) + \frac{t_{k+1} - t}{\mathcal{T}_k} \Omega_2(\mathcal{T}_k) \right\} \xi(t). \end{aligned} \tag{29}$$

Therefore, based on conditions (12) and (13), one obtains

$$\dot{\mathcal{W}}(t) + 2\alpha \mathcal{W}(t) < 0, \quad t \in (t_k^+, t_{k+1}]. \tag{30}$$

Pre- and post-multiply inequality (9) by  $\text{diag} \{ I, P^{-1} \}$ ,

$$\begin{bmatrix} P_1 & I + \mathcal{Q} \\ \star & P_1^{-1} \end{bmatrix} > 0. \tag{31}$$

Hence, one can derive

$$\begin{aligned} \mathcal{W}(t_k^+) &= \mathcal{V}_1(t_k^+) + \mathcal{V}_2(t_k^+) \\ &\leq z^T(t_k) P_1 z(t_k) + \mathcal{V}_2(t_k^-) \\ &= \mathcal{W}(t_k), \end{aligned} \tag{32}$$

which means that the jumps of  $\mathcal{W}(t)$  at every impulse instant are decreasing, that is,  $\mathcal{W}(t_k^+) < \mathcal{W}(t_k)$ .

For  $t \in (t_k^+, t_{k+1}]$ , it follows from Lemma 1 that

$$\begin{aligned} \mathcal{W}(t) &\leq e^{-2\alpha(t-t_k)} \mathcal{W}(t_k) \\ &\leq e^{-2\alpha(t-t_{k-1})} \mathcal{W}(t_{k-1}) \\ &\leq \dots \\ &\leq e^{-2\alpha t} \mathcal{W}(0). \end{aligned} \tag{33}$$

On the one hand, we can know

$$\begin{aligned} \mathcal{W}(0) &= z^T(0) P_1 z(0) + \int_{-\tau(0)}^0 e^{2\alpha s} z^T(s) P_2 z(s) ds \\ &\leq \theta_3 \sup_{s \in [-\tau, 0]} \|\varphi(s)\|^2, \end{aligned} \tag{34}$$

where  $\theta_3 = \lambda_{\max}(P_1) + \tau \cdot \lambda_{\max}(P_2)$ .

On the other hand, from Lemma 2 and (34), one gets

$$\|z(t)\|^2$$

$$\begin{aligned}
 &\leq \theta_1 \|z(t_k)\|^2 + \theta_2 \int_{t_k-\tau(t_k)}^{t_k} \|z(s)\|^2 ds \\
 &< \max \left\{ \frac{\theta_1}{\lambda_{\min}(P_1)}, \frac{\theta_2 e^{2\alpha\tau}}{\lambda_{\min}(P_2)} \right\} \mathcal{W}(t_k) \\
 &< \max \left\{ \frac{\theta_1}{\lambda_{\min}(P_1)}, \frac{\theta_2 e^{2\alpha\tau}}{\lambda_{\min}(P_2)} \right\} e^{-2\alpha t_k} \mathcal{W}(0) \\
 &\leq e^{2\alpha T_M} \max \left\{ \frac{\theta_1}{\lambda_{\min}(P_1)}, \frac{\theta_2 e^{2\alpha\tau}}{\lambda_{\min}(P_2)} \right\} e^{-2\alpha t} \mathcal{W}(0) \\
 &\leq e^{2\alpha T_M} \max \left\{ \frac{\theta_1}{\lambda_{\min}(P_1)}, \frac{\theta_2 e^{2\alpha\tau}}{\lambda_{\min}(P_2)} \right\} \theta_3 \\
 &\times e^{-2\alpha t} \sup_{s \in [-\tau, 0]} \|\varphi(s)\|^2. \tag{35}
 \end{aligned}$$

Thus, we can obtain

$$\|z(t)\| \leq \epsilon e^{-\alpha t} \sup_{s \in [-\tau, 0]} \|\varphi(s)\|, \tag{36}$$

where

$$\epsilon = e^{\alpha T_M} \sqrt{\max \left\{ \frac{\theta_1}{\lambda_{\min}(P_1)}, \frac{\theta_2 e^{2\alpha\tau}}{\lambda_{\min}(P_2)} \right\} \theta_1}.$$

Then, the exponential stabilization of system (3) can be achieved. This completes the proof.

*Remark 1* Although the Lyapunov functional  $V_1(t)$  and  $V_2(t)$  are positive definite, the IBBLF  $\mathcal{W}(t)$  may not be so. Therefore, the IBBLF approach relaxes the requirement of positive definiteness and it only satisfies  $\mathcal{W}(t)$  is positive at the moment of impulsive  $t = t_k$  ( $t = t_k^-$ ). In addition,  $\dot{\mathcal{W}}(t) < 0$  can be obtained by using IBBLF, it is obvious that one can ensure  $\mathcal{W}(t)$  is decreasing on the impulsive instants.

*Remark 2* In (14), the IBBLF  $\sum_{l=3}^7 V_l(t, z(t))$ , takes full advantage of the state information from  $z(t_k^+)$  to  $z(t)$  and  $z(t)$  to  $z(t_{k+1})$ , which not only can obtain less conservative results, but also improve the interval  $[\mathcal{T}_m, \mathcal{T}_M]$  of allowable aperiodic impulses compared with the LFM in Refs. [28,45,46].

### 3.2 Application: exponential stability of SDSs with variable sampling

According to system (1), we consider the following SDSs:

$$\begin{cases} \dot{z}(t) = \mathcal{A}z(t) + \mathcal{B}g(z(t)) + \mathcal{C}h(z(t-\tau(t))) + u_c(t), \\ z(s) = \varphi(s), \quad s \in [-\tau, 0], \end{cases} \tag{37}$$

where  $u_c(t) = \mathcal{K}z(t_k)$ , and the other notations have the same meaning as Theorem 1. In order to use the results of Theorem 1, the SDSs can be written as an impulsive system with state  $\omega(t) := \text{col}\{z(t), x(t)\}$  and  $x(t) := z(t_k)$ ,  $t \in (t_k, t_{k+1}]$  and  $\mathcal{T}_k = t_{k+1} - t_k \in [\mathcal{T}_m, \mathcal{T}_M]$ . The dynamics of system (38) can be written as

$$\begin{cases} \dot{\omega}(t) = \mathfrak{A}\omega(t) + \mathfrak{B}\tilde{g}(\omega(t)) + \mathfrak{C}\tilde{h}(\omega(t-\tau(t))), \quad t \neq t_k, \\ \omega(t_k^+) = \begin{bmatrix} z(t_k^-) \\ z(t_k^-) \end{bmatrix}, \quad t = t_k, \quad \forall k \in \mathbb{N}^+, \end{cases} \tag{38}$$

where

$$\begin{aligned}
 \mathfrak{A} &= \begin{bmatrix} \mathcal{A} & \mathcal{K} \\ 0 & 0 \end{bmatrix}, \quad \mathfrak{B} = \begin{bmatrix} \mathcal{B} & 0 \\ 0 & 0 \end{bmatrix}, \quad \mathfrak{C} = \begin{bmatrix} \mathcal{C} & 0 \\ 0 & 0 \end{bmatrix}, \\
 \tilde{g}(\omega(t)) &= \begin{bmatrix} g(z(t)) \\ g(x(t)) \end{bmatrix}, \quad \tilde{h}(\omega(t-\tau(t))) = \begin{bmatrix} h(z(t-\tau(t))) \\ h(x(t-\tau(t))) \end{bmatrix}.
 \end{aligned}$$

and the initial condition  $z(s) = \varphi(s)$ ,  $s \in [-\tau, 0]$ .

Between the impulses  $z(t)$ ,  $x(t)$  evolve according to (37) and at the impulse instant  $t_k$ , the value of  $z(t)$  before and after  $t_k$  remains unchanged, but the value of  $x(t)$  is updated by  $x(t_k^-)$ . Then exponential stability of SDSs (38) can be obtained as follows:

**Theorem 2** *Given constants  $\mathcal{T}_m > 0$ ,  $\mathcal{T}_M > 0$ ,  $\alpha > 0$ ,  $\varepsilon_1, \varepsilon_2$ , if there exist matrices  $P_j > 0$ ,  $X_j > 0$ ,  $M_1 > 0$ ,  $N_1 > 0$ , diagonal matrices  $\Lambda_j > 0$ , symmetric matrix  $S$  and arbitrary matrices  $Q_j, R, L, \mathcal{D}_j, Y_\iota, Z_\iota, M_\kappa, N_\kappa$ ,  $j = 1, 2, \iota = 1, 2, 3, \kappa = 2, 3$ , such that conditions (10) (11) of the Theorem 1 and following LMIs hold for  $\mathcal{T}_k \in [\mathcal{T}_m, \mathcal{T}_M]$ :*

$$\tilde{\Omega}_1(\mathcal{T}_k) = \tilde{\Xi}_1 + \mathcal{T}_k \tilde{\Xi}_2 < 0, \tag{39}$$

$$\tilde{\Omega}_2(\mathcal{T}_k) = \tilde{\Xi}_1 + \mathcal{T}_k \tilde{\Xi}_3 < 0. \tag{40}$$

*Then, the system (38) is exponential stable and the gain matrix can be obtained by  $\mathcal{K} = (\mathcal{D}^T)^{-1} \tilde{\mathcal{K}}$ . The process of proof is shown in Appendix B, C.*

*Remark 3* What's worth noting here is that  $\mathcal{W}(t)$  is strictly monotonically decreasing due to  $\dot{\mathcal{W}}(t) < 0$ ,  $(t_k^+, t_{k+1}]$ . In [38], discrete Lyapunov stability theory and discrete integral method was proposed to prove the asymptotically stable of linear SDSs. Unfortunately, these analysis methods cannot be used to discuss nonlinear SDSs. However, to bridge the generation gap, discrete-time Lyapunov theorem and Lemma 2 are



developed to derive the exponential stability conditions.

### 4 Numerical simulations

The point of this part is that we use two numerical examples to illustrate the less conservatism and effectiveness of the proposed approach in this work.

#### 4.1 Example 1

For comparison with the Ref. [41], the system is reduced to a linear impulsive system as follows:

$$\begin{cases} \dot{z}(t) = \mathcal{A}z(t), & t \neq t_k, \\ z(t_k^+) = \mathcal{Q}z(t_k), & t = t_k. \end{cases} \tag{41}$$

Namely, for system (3), the matrices  $\mathcal{B} = \mathcal{C} = \Gamma = 0$ . We consider the asymptotically stable of the system (42) in the following two cases.

*Case 1* When  $\mathcal{A}$  and  $\mathcal{Q}$  are set to the following matrices:

$$\mathcal{A} = \begin{bmatrix} -3.5 & 0.3 \\ 0.1 & 0.6 \end{bmatrix}, \quad \mathcal{Q} = \begin{bmatrix} 1.3 & 0.1 \\ 0.1 & 0.01 \end{bmatrix}.$$

One can know that the eigenvalues of  $\mathcal{A}$  are  $-3.50489$  and  $0.6049$ , meanwhile, the eigenvalues of  $\mathcal{Q}$  are  $1.3077$  and  $0.0023$ . The impulsive system can't achieve stable if the impulsive interval is too small or too large. Thus,  $\mathcal{T}_k$  plays a vital part for the stability of system (42). By using the theoretical results of Theorem 1, the allowable impulsive interval is listed in Table 1 compare with Refs. [41–44]. From Table 1, it is obviously that the impulsive interval obtained by Theorem 1 is better than Refs. [41–44], which indicates that the results of Theorem 1 is less conservative. However, the cost of computational complexity is large than Refs. [41–43] (Note: The presence of “NDVs” in Table 2 means the number of decision variables).

*Case 2* When we set the matrices  $\mathcal{A}$  and  $\mathcal{Q}$  as follows:

$$\mathcal{A} = \begin{bmatrix} 1 & 3 \\ -1 & 2 \end{bmatrix}, \quad \mathcal{Q} = \begin{bmatrix} 0.5 & 0 \\ 0 & 0.5 \end{bmatrix}.$$

$\mathcal{A}$  is anti-Hurwitz and  $\mathcal{Q}$  is Schur, the dwell-time  $\mathcal{T}_k$  should be small enough to guarantee the stability of system (42). When the dwell-time  $\mathcal{T}_k < \mathcal{T}$ , the impulsive system is asymptotical stable, where  $\mathcal{T}$  denotes the maximal dwell-time. Further, by using Theorem 1,  $\mathcal{T}$

**Table 2** Allowable intervals  $[\mathcal{T}_m, \mathcal{T}_M]$  with aperiodic impulses

Methods	Intervals	NDVs
[41]	[0.0802, 1.2082]	$5n^2 + 2n$
[43]	[0.0780, 2.3214]	$9.5n^2 + 3.5n$
[42]	[0.0780, 2.6417]	$23.5n^2 + 1.5n$
[44]	[0.0780, 2.8056]	$178.5n^2 + 3.5n$
Theorem 1 ( $\mathcal{D}_1 = 0$ )	[0.0780, 3.3064]	$25.5n^2 + 3.5n$
Theorem 1 ( $\mathcal{D}_1 \neq 0$ )	[0.0780, 4.8474]	$26.5n^2 + 3.5n$

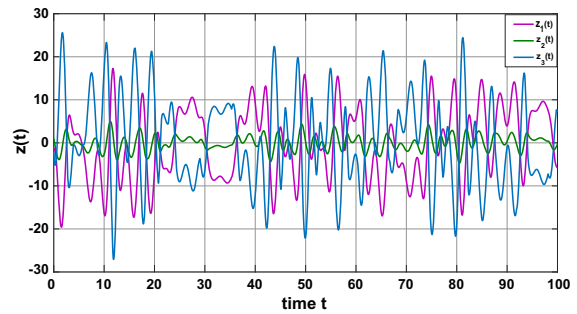


**Fig. 1** State trajectory of system (1) without any controller

can be obtained (See Table 3). It is clear that  $\mathcal{T}$  obtained by this work is larger than Refs. [41–43], thus the results of Theorem 1 has less conservatism than [41–43].

#### 4.2 Example 2

Consider the DNNs with the following parameters:

$$\mathcal{A} = \begin{bmatrix} -1 & 0 & 0 \\ 0 & -1 & 0 \\ 0 & 0 & -1 \end{bmatrix}, \quad \mathcal{B} = \begin{bmatrix} 0 & 8 & 0 \\ 1 & 0 & 1 \\ 0 & -11 & 1 \end{bmatrix}, \quad \mathcal{C} = \begin{bmatrix} 2 & 0 & 0 \\ 0.2 & 0.1 & 0 \\ 9 & 0 & 0.1 \end{bmatrix}.$$

Select  $\tau(t) = 0.3 + 0.2sint$ ,  $g(z(t)) = z(t)$ ,  $h(z(t)) = 0.5(|z + 1| - |z - 1|)$ , thus  $\mathcal{G} = \mathcal{H} = \text{diag}\{1, 1, 1\}$ . Figure 1 draws the state trajectory  $z(t)$  without controller under the initial condition  $\varphi(s) = [-2, 1, -2]^T$ ,  $s \in [-0.5, 0]$ . Obviously, system (1) is unstable without controller.

Next, we will use these parameters to analyze the impulsive DNNs and SDSs, respectively.

*Case 1: Impulsive DNNs (3)* We verify the relation of the exponential rate  $\alpha$  and  $\mathcal{T}_M$  under different impulse strength. Table 4 shows the maximum allowable bound for  $\mathcal{T}_M$  with  $\mathcal{T}_m = 0.001$ . Figure 2 depicts the state trajectory of DNNs with stable impulse.



**Table 3** Maximal dwell-time  $\mathcal{T}_k$  with aperiodic impulses

Methods	[41]	[43]	[42]	Theorem 1
$\mathcal{T}$	0.4471	0.4483	0.4618	0.6574
Improvement(%)	47.03	46.64	42.35	--

**Table 4** Allowable upper bound  $\mathcal{T}_M$  when  $\mathcal{T}_m = 0.001$  for different  $\alpha$

$\alpha$	0.1	0.3	0.5	0.7	0.9
$\mathcal{Q} = -0.5I$	0.5575	0.5395	0.5209	0.5019	0.4745
$\mathcal{Q} = -0.9I$	0.5577	0.5402	0.5213	0.5021	0.4748

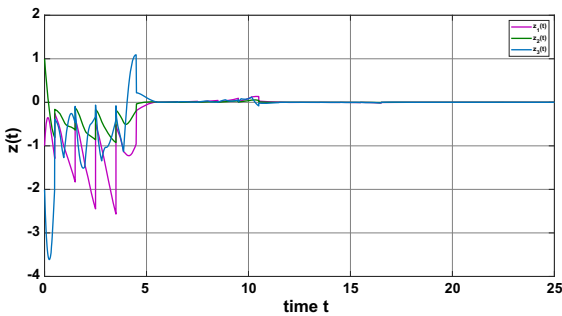


**Fig. 2** State trajectory of system (1) with stable impulses

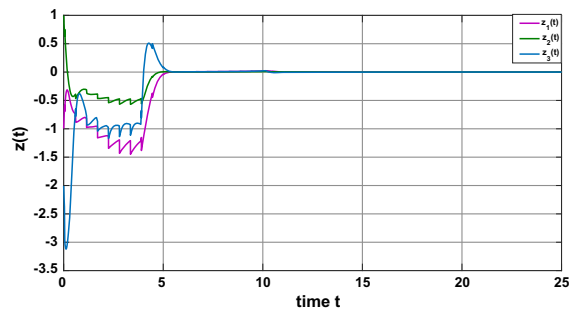


**Fig. 3** State trajectory of system (1) with unstable impulses

*Remark 4* Fig. 3 describes the state trajectory of system (1) with unstable impulsive. As can be seen from the Fig. 3 (where  $\mathcal{Q} = \text{diag}\{0.2, 0.2, 0.2\}$ , that is  $z(t_k^+) = 1.2z(t_k)$ ), the system can still achieve stability under the action of the impulsive controller (2). The reason of this stability is that the feedback term is incorporated into the controller. Namely, the feedback controller plays a meaningful role when the unstable impulses are activated. But in Refs. [25,49], when the unstable impulses was activated, they can't obtain the expected results because the feedback control was not considered. Thus, the hybrid controller presented in this work is more general than the previous works. In order to verify the influence of  $u_1(t)$  in the hybrid controller (2), we set  $\Gamma = 0$  when  $\mathcal{Q} = 0.1I$ . From Fig. 4, the exponential stability can't be achieved, which further demonstrates the feedback control  $u_1(t)$  in hybrid controller (2) has an important significance in the exponentially stable.

*Case 2: SDSs (38)* Firstly, in (39), the controller  $u_c(t) = \mathcal{K}z(t_k)$  and the delay  $\tau(t) = \tau$  is constant delay. To describe the validity of the results of Theorem

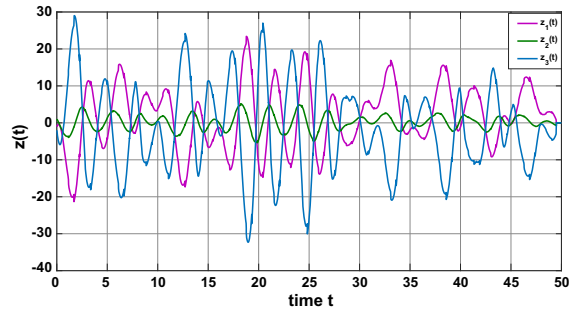


**Fig. 4** State trajectory of system (1) with unstable impulses

2, the comparisons results are obtained. The maximum allowable bound for  $\mathcal{T}_M$  with  $\mathcal{T}_m = 10^{-5}$  is shown in Table 5. Additionally, the number of decision variables are also compared, which is a measure of computational complexity. Therefore, Table 5 displays that when the computational complexity increases, a relatively conservative result is obtained than those Refs. [28,45,46].

Secondly, set  $\alpha = 0.8$ ,  $\mathcal{T}_m = 0.001$ ,  $\mathcal{T}_M = 0.3790$ , then the feasible solution of Theorem 2 can be got by MATLAB LMI Toolbox, and the following gain matrix

**Table 5** The maximum allowable upper bound  $\mathcal{T}_M$  with  $\mathcal{T}_m = 10^{-5}$

Methods	$\mathcal{T}_M$	NDV
[28], [45], [46]	0.1348	$8.5n^2 + 3.5n$
Theorem 2 ( $\mathcal{D}_1 = 0$ )	0.5207	$25.5n^2 + 3.5n$
Theorem 2 ( $\mathcal{D}_1 \neq 0$ )	0.5216	$26.5n^2 + 3.5n$

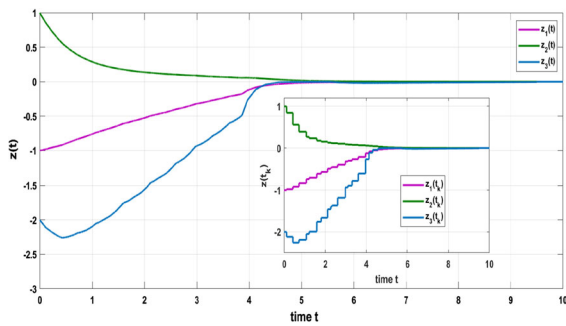


**Fig. 5** State trajectory of system (1) with sampled-data controller

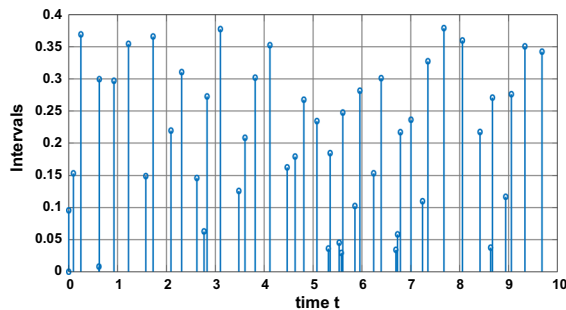


**Fig. 6** Sampling instants and sampling periods

$\mathcal{K}$  can be obtained

$$\mathcal{K} = \begin{bmatrix} -0.6212 & -0.2322 & -0.3941 \\ 0.0311 & -0.3344 & -0.1689 \\ 1.0447 & 0.6187 & -3.2544 \end{bmatrix}.$$

And consider  $\varphi(s) = [-2, 1, -2]^T$ ,  $s \in [-0.5, 0]$ . The state trajectory  $z(t)$ , sampled-data state  $z(t_k)$ , and sampling instants and sampling periods under aperiodic sampling is described in Figs. 5 and 6, respectively, which shows the exponentially stable can be achieved by the sampled-data controller.

### 5 Conclusion

This work studies the analysis of the exponential stability for DNNs based on a hybrid control strategy, where unstable and stable impulses have all been considered. An exponential stability criterion for DNNs by employing an improved IBBLF with discontinuity at the impulses instant has been obtained. Then, sufficient conditions have been obtained on the ranged dwell-time, which is the result of stability in discrete-time, but expressed in continuous-time. Lastly, the derived results have also been applied to SDSs and the corresponding stability results are also obtained. In our future work, the following topics will be considered: 1. Consider the case that the delay-impulses between two consecutive impulsive instants based on the IBBLF method. 2. Design a novel event-triggered control with the aid of IBBLF, where the impulsive sequence is unknown sequence and determined by the event-triggered condition.

**Acknowledgements** This work was supported by the National Natural Science Foundation of China under Grant (Nos. 61703060, 12061088, 61802036 and 61873305), the Sichuan Science and Technology Program under Grant No. 21YYJC0469, the Project funded by China Postdoctoral Science Foundation under Grant Nos. 2020 M683274 and 2021T140092, Supported by the Open Research Project of the State Key Laboratory of Industrial Control Technology, Zhejiang University,China (No. ICT2021B38), Guangdong Basic and Applied Basic Research Foundation (2021A1515011692).

**Data availability** All data generated or analyzed during this study are included in this article.

### Declarations

**Conflict of interest** We declare that we do not have any commercial or associative interest that represents a conflict of interest in connection with the work submitted.

### Appendix

#### Appendix A

$$\begin{aligned} \Xi_1 &= e_1^T P_2 e_1 - (1-\mu)e^{-2\alpha\tau} e_2^T P_2 e_2 - \Phi_5^T \mathcal{L}_1 \Phi_5 - \Phi_6^T \mathcal{L}_2 \\ &\times \Phi_6 + He\{e_1^T P_1 e_5 + \alpha e_1^T P_1 e_1 + \Sigma_6^T Q_1 \Sigma_1 + \Sigma_6^T \\ &\times Q_2 \Sigma_2 + e_5^T R(e_1 - e_4) + (e_1 - (I + \mathcal{D})e_3)Re_5 \\ &\quad + 2\alpha(e_1 - (I + \mathcal{D})e_3)R(e_1 - e_4) + e_8^T \Lambda_1 (\mathcal{G}e_1 - e_8) \end{aligned}$$

$$\begin{aligned}
 & +e_9^T \Lambda_2(\mathcal{H}e_2 - e_9) + \Phi_7^T \Phi_8\}, \\
 \Xi_2 = & \Sigma_8^T Q_1 \Sigma_1 + \Sigma_8^T Q_2 \Sigma_2 + \Sigma_5^T Q_2 \Sigma_3 + 2\alpha \Sigma_5^T Q_1 \Sigma_1 \\
 & + 2\alpha \Sigma_5^T Q_2 \Sigma_2 - \Sigma_1^T S \Sigma_1 + \mathcal{T}_M e_5^T X_2 e_5 + \Phi_1 + \Phi_3 \\
 & - e^{-2\alpha \mathcal{T}_M} e_6^T M_1 e_6 + \frac{\alpha}{2} \mathcal{T}_{\max} \Sigma_1^T S \Sigma_1, \\
 \Xi_3 = & \Sigma_7^T Q_1 \Sigma_1 + \Sigma_7^T Q_2 \Sigma_2 + \Sigma_4^T Q_2 \Sigma_3 + 2\alpha \Sigma_4^T Q_1 \Sigma_1 \\
 & + 2\alpha \Sigma_4^T Q_2 \Sigma_2 + \Sigma_1^T S \Sigma_1 + \mathcal{T}_M e_5^T X_1 e_5 + \Phi_2 + \Phi_4 \\
 & - e_7^T N_1 e_7 + \frac{\alpha}{2} \mathcal{T}_{\max} \Sigma_1^T S \Sigma_1, \\
 \Sigma_1 = & \text{col}\{(I + \mathcal{D})e_3, e_4\}, \Sigma_2 = \text{col}\{e_1 - (I + \mathcal{D})e_3, e_1 - e_4\}, \\
 \Sigma_3 = & \{e_5, e_5\}, \Sigma_4 = \text{col}\{e_1 - (I + \mathcal{D})e_3, 0\}, \\
 \Sigma_5 = & \text{col}\{0, e_1 - e_4\}, \Sigma_6 = \text{col}\{(I + \mathcal{D})e_3 - e_1, e_1 - e_4\}, \\
 \Sigma_7 = & \text{col}\{e_5, 0\}, \Sigma_8 = \text{col}\{0, e_5\},
 \end{aligned}$$

$$\begin{aligned}
 \Phi_1 = & -e^{-2\alpha \mathcal{T}_M} \{e_3^T M_2 e_3 + e_4^T M_3 e_4 + He\{e_6^T Y_1 e_3 \\
 & + e_6^T Y_2 e_4 + e_3^T Y_3 e_4\}\}, \\
 \Phi_2 = & e_1^T M_1 e_1 + e_3^T M_2 e_3 + e_4^T M_3 e_4 + He\{e_1^T Y_1 e_3 \\
 & + e_1^T Y_2 e_4 + e_3^T Y_3 e_4\}, \\
 \Phi_3 = & e_1^T N_1 e_1 + e_3^T N_2 e_3 + e_4^T N_3 e_4 + He\{e_1^T Z_1 e_3 \\
 & + e_1^T Z_2 e_4 + e_3^T Z_3 e_4\}, \\
 \Phi_4 = & -e_3^T N_2 e_3 - e_4^T N_3 e_4 - He\{e_7^T Z_1 e_3 + e_7^T Z_2 e_4 + e_3^T Z_3 e_4\}, \\
 \Phi_5 = & \text{col}\{e^{-\alpha \mathcal{T}_M} (e_1 - e_3), e_4 - e_1\}, \Phi_7 = \mathcal{D}_1 e_1 + \mathcal{D}_2 e_5, \\
 \Phi_6 = & \text{col}\{e^{-\alpha \mathcal{T}_M} (e_1 + e_3 - 2e_6), e_1 + e_4 - 2e_7\}, \\
 \Phi_8 = & -e_5 + (\mathcal{A} - \Gamma)e_1 + \mathcal{B}e_8 + \mathcal{C}e_9.
 \end{aligned}$$

Appendix B: Proof of Theorem 2

*Proof Step 1* Construct the following LKFs:

$$\begin{aligned}
 \mathcal{V}_1(t) = & \omega^T(t) \tilde{P}_1 \omega(t), \\
 \mathcal{V}_2(t) = & \int_{t-\tau(t)}^t e^{2\alpha(s-t)} \omega^T(s) \tilde{P}_2 \omega(s) ds, \\
 \mathcal{V}_3(t) = & 2\tilde{\eta}_3^T(t) [\tilde{Q}_1 \tilde{\eta}_1(t) + \tilde{Q}_2 \tilde{\eta}_2(t)], \\
 \mathcal{V}_4(t) = & 2[\omega(t) - \omega(t_k)]^T \tilde{R} [\omega(t) - \omega(t_{k+1})], \\
 \mathcal{V}_5(t) = & (t_{k+1} - t)(t - t_k) \tilde{\eta}_1^T(t) \tilde{S} \tilde{\eta}_1(t), \\
 \mathcal{V}_6(t) = & (t_{k+1} - t)(t_{k+1} - t_k) \int_{t_k}^t e^{2\alpha(s-t)} \dot{\omega}^T(s) \tilde{X}_1 \dot{\omega}(s) ds \\
 & - (t - t_k)(t_{k+1} - t_k) \int_t^{t_{k+1}} e^{2\alpha(s-t)} \dot{\omega}^T(s) \tilde{X}_2 \dot{\omega}(s) ds,
 \end{aligned}$$

$$\begin{aligned}
 \mathcal{V}_7(t) = & (t_{k+1} - t) \int_{t_k}^t e^{2\alpha(s-t)} \tilde{\eta}_4^T(s) \tilde{\mathcal{M}} \tilde{\eta}_4(s) ds \\
 & - (t - t_k) \int_t^{t_{k+1}} e^{2\alpha(s-t)} \tilde{\eta}_4^T(s) \tilde{\mathcal{N}} \tilde{\eta}_4(s) ds,
 \end{aligned}$$

where define  $\mathfrak{R} = [? \ 0; 0 \ 0]$ , thus  $\mathfrak{R} = \tilde{P}_j$  when  $? = P_j$ ,  $\mathfrak{R} = \tilde{X}_j$  when  $? = X_j$ ,  $\mathfrak{R} = \tilde{D}_j$  when  $? = \mathcal{D}_j$  and  $\mathfrak{R} = \tilde{R}$  when  $? = R, j = 1, 2$ .

$$\begin{aligned}
 \tilde{Q}_i = & \begin{bmatrix} Q_{i1} & 0 & Q_{i2} & 0 \\ 0 & 0 & 0 & 0 \\ Q_{i3} & 0 & Q_{i4} & 0 \\ 0 & 0 & 0 & 0 \end{bmatrix}, \tilde{S} = \begin{bmatrix} S_{11} & 0 & S_{12} & 0 \\ 0 & 0 & 0 & 0 \\ S_{21} & 0 & S_{22} & 0 \\ 0 & 0 & 0 & 0 \end{bmatrix}, \\
 \tilde{\mathcal{M}} = & \begin{bmatrix} M_1 & Y_1 & Y_2 & 0 \\ \star & M_2 & Y_3 & 0 \\ \star & \star & M_3 & 0 \\ \star & \star & \star & 0 \end{bmatrix}, \tilde{\mathcal{N}} = \begin{bmatrix} N_1 & Z_1 & Z_2 & 0 \\ \star & N_2 & Z_3 & 0 \\ \star & \star & N_3 & 0 \\ \star & \star & \star & 0 \end{bmatrix}.
 \end{aligned}$$

The other symbols are defined in Appendix C. In addition, the process of proof is similar to Theorem 1, so it is omitted here.

*Step 2* In order to obtain gain matrix  $\mathcal{K}$ , define  $\mathcal{D}_1 = \varepsilon_1 \mathcal{D}, \mathcal{D}_2 = \varepsilon_2 \mathcal{D}$ , and we introduce a variable  $\tilde{\mathcal{K}} = (\mathcal{D}^T) \mathcal{K}$ , thus  $\mathcal{K} = (\mathcal{D}^T)^{-1} \tilde{\mathcal{K}}$ .

Appendix C

$$\begin{aligned}
 \tilde{\pi}_1(t) = & \frac{1}{t-t_k} \int_{t_k}^t \omega(s) ds, \tilde{\pi}_2(t) = \frac{1}{t_{k+1}-t} \int_t^{t_{k+1}} \omega(s) ds, \\
 \tilde{\eta}_1(t) = & \text{col}\{\omega(t_k), \omega(t_{k+1})\}, \tilde{\eta}_4(t) = \text{col}\{\omega(t), \omega(t_{k+1})\}, \\
 \tilde{\eta}_2(t) = & \text{col}\{\omega(t) - \omega(t_k), \omega(t) - \omega(t_{k+1})\}, \\
 \tilde{\eta}_3(t) = & \text{col}\{(t_{k+1}-t)(\omega(t) - \omega(t_k)), (t-t_k)(\omega(t) - \omega(t_{k+1}))\}, \\
 \tilde{\eta}_5(t) = & \text{col}\{\tilde{\pi}_1(t), \tilde{\pi}_2(t), \tilde{g}(\omega(t)), \tilde{h}(\omega(t - \tau(t)))\}, \\
 \tilde{\xi}(t) = & \text{col}\{\omega(t), \omega(t - \tau(t)), \tilde{\eta}_1(t), \dot{\omega}(t), \tilde{\eta}_5(t)\}, \iota = 1, 2, 3, \\
 \tilde{M}_\iota = & \begin{bmatrix} M_\iota & 0 \\ 0 & 0 \end{bmatrix}, \tilde{N}_\iota = \begin{bmatrix} N_\iota & 0 \\ 0 & 0 \end{bmatrix}, \tilde{Y}_\iota = \begin{bmatrix} Y_\iota & 0 \\ 0 & 0 \end{bmatrix}, \tilde{Z}_\iota = \begin{bmatrix} Z_\iota & 0 \\ 0 & 0 \end{bmatrix}, \\
 \tilde{\Xi}_1 = & e_1^T \tilde{P}_2 e_1 - (1 - \mu) e^{-2\alpha \tau} e_2^T \tilde{P}_2 e_2 - \tilde{\Phi}_5^T \mathcal{L}_1 \tilde{\Phi}_5 \\
 & - \tilde{\Phi}_6^T \mathcal{L}_2 \tilde{\Phi}_6 + He\{e_1^T \tilde{P}_1 e_5 + \alpha e_1^T \tilde{P}_1 e_1 + \Sigma_6^T \\
 & \times \tilde{Q}_1 \Sigma_1 + \Sigma_6^T \tilde{Q}_2 \Sigma_2 + e_5^T \tilde{R} (e_1 - e_4) + (e_1 \\
 & - e_3)^T \tilde{R} e_5 + 2\alpha (e_1 - e_3)^T \tilde{R} (e_1 - e_4) + e_8^T \\
 & \times \Lambda_1 (\mathcal{G}e_1 - e_8) + e_9^T \Lambda_2 (\mathcal{H}e_2 - e_9) + \tilde{\Phi}_7^T \tilde{\Phi}_8\}, \\
 \tilde{\Xi}_2 = & \Sigma_8^T \tilde{Q}_1 \Sigma_1 + \Sigma_8^T \tilde{Q}_2 \Sigma_2 + \Sigma_5^T \tilde{Q}_2 \Sigma_3 + 2\alpha \Sigma_5^T \tilde{Q}_1 \\
 & \times \Sigma_1 + 2\alpha \Sigma_5^T \tilde{Q}_2 \Sigma_2 - \Sigma_1^T \tilde{S} \Sigma_1 + \mathcal{T}_M e_5^T \tilde{X}_2 e_5
 \end{aligned}$$

$$\begin{aligned}
& + \tilde{\Phi}_1 + \tilde{\Phi}_3 - e^{2\alpha\mathcal{T}_M} e_6^T \tilde{M}_1 e_6 + \frac{\alpha}{2} \mathcal{T}_M \Sigma_1^T \tilde{S} \Sigma_1, \\
\tilde{\Xi}_3 = & \Sigma_7^T \tilde{Q}_1 \Sigma_1 + \Sigma_7^T \tilde{Q}_2 \Sigma_2 + \Sigma_4^T \tilde{Q}_2 \Sigma_3 + 2\alpha \Sigma_4^T \tilde{Q}_1 \\
& \times \Sigma_1 + 2\alpha \Sigma_4^T \tilde{Q}_2 \Sigma_2 + \Sigma_1^T \tilde{S} \Sigma_1 + \mathcal{T}_M e_5^T \tilde{X}_1 e_5 \\
& + \tilde{\Phi}_2 + \tilde{\Phi}_4 - e_7^T \tilde{N}_1 e_7 + \frac{\alpha}{2} \mathcal{T}_M \Sigma_1^T \tilde{S} \Sigma_1, \\
\Sigma_1 = & \text{col}\{e_3, e_4\}, \quad \Sigma_2 = \text{col}\{e_1 - e_3, e_1 - e_4\}, \\
\Sigma_3 = & \text{col}\{e_5, e_5\}, \quad \Sigma_4 = \text{col}\{e_1 - e_3, 0\}, \\
\Sigma_5 = & \text{col}\{0, e_1 - e_4\}, \quad \Sigma_7 = \text{col}\{e_5, 0\}, \\
\Sigma_6 = & \text{col}\{e_3 - e_1, e_1 - e_4\}, \quad \Sigma_8 = \text{col}\{0, e_5\}, \\
\tilde{\Phi}_1 = & -e^{-2\alpha\mathcal{T}_M} \{e_3^T \tilde{M}_2 e_3 + e_4^T \tilde{M}_3 e_4 + He\{e_6^T \tilde{Y}_1 e_3 \\
& + e_6^T \tilde{Y}_2 e_4 + e_3^T \tilde{Y}_3 e_4\}\}, \\
\tilde{\Phi}_2 = & e_1^T \tilde{M}_1 e_1 + e_3^T \tilde{M}_2 e_3 + e_4^T \tilde{M}_3 e_4 + He\{e_1^T \tilde{Y}_1 e_3 \\
& + e_1^T \tilde{Y}_2 e_4 + e_3^T \tilde{Y}_3 e_4\}, \\
\tilde{\Phi}_3 = & e_1^T \tilde{N}_1 e_1 + e_3^T \tilde{N}_2 e_3 + e_4^T \tilde{N}_3 e_4 + He\{e_1^T \tilde{Z}_1 e_3 \\
& + e_1^T \tilde{Z}_2 e_4 + e_3^T \tilde{Z}_3 e_4\}, \\
\tilde{\Phi}_4 = & -e_3^T \tilde{N}_2 e_3 - e_4^T \tilde{N}_3 e_4 - He\{e_7^T \tilde{Z}_1 e_3 + e_7^T \tilde{Z}_2 e_4 \\
& + e_3^T \tilde{Z}_3 e_4\}, \\
\tilde{\Phi}_5 = & \text{col}\{e^{-\alpha\mathcal{T}_M} (e_1 - e_3), e_4 - e_1\}, \\
\tilde{\Phi}_6 = & \text{col}\{e^{-\alpha\mathcal{T}_M} (e_1 + e_3 - 2e_6), e_1 + e_4 - 2e_7\}, \\
\tilde{\Phi}_7 = & \tilde{D}_1 e_1 + \tilde{D}_2 e_5, \quad \tilde{\Phi}_8 = -e_5 + \mathfrak{A}e_1 + \mathfrak{B}e_8 + \mathfrak{C}e_9.
\end{aligned}$$

## References

- Zhang, Y., Wang, X., Friedman, E.G.: Memristor-based circuit design for multilayer neural networks. *IEEE Trans. Circuits Syst. I, Reg. Papers* **65**(2), 677–686 (2018)
- Song, Q., Chen, S., Zhao, Z., Liu, Y., Alsaadi, F.E.: Passive filter design for fractional-order quaternion-valued neural networks with neutral delays and external disturbance. *Neural Netw.* **137**, 18–30 (2021)
- Dong, S., Zhong, S., Shi, K., Kang, W., Cheng, J.: Further improved results on non-fragile  $H_\infty$  performance state estimation for delayed static neural networks. *Neurocomputing* **356**, 9–20 (2019)
- Dong, S., Zhu, H., Zhong, S., Shi, K., Liu, Y.: New study on fixed-time synchronization control of delayed inertial memristive neural networks. *Appl. Math. Comput.* **399**, 126035 (2021)
- Xiao, J., Cheng, J., Shi, K., Zhang, R.: A general approach to fixed-time synchronization problem for fractional-order multi-dimension-valued fuzzy neural networks based on memristor. *IEEE Trans. Fuzzy Syst.* (2021). <https://doi.org/10.1109/TFUZZ.2021.3051308>
- Guo, D., Perc, M.C.V., Zhang, Y., Xu, P., Yao, D.: Frequency-difference-dependent stochastic resonance in neural systems. *Phys. Rev. E* **96**, 022415 (2017)
- Fister, I., Suganthan, P.N., Kamal, S.M., Al-Marzouki, F.M., Perc, M., Strnad, D.: Artificial neural network regression as a local search heuristic for ensemble strategies in differential evolution. *Nonlinear Dyn.* **84**(2), 895–914 (2016)
- Erkaymaz, O.: Resilient back-propagation approach in small-world feed-forward neural network topology based on newman-watts algorithm. *Neural Comput. Appl.* **32**(20), 16279–16289 (2020)
- Lin, W., He, Y., Zhang, C., Wu, M., Shen, J.: Extended dissipativity analysis for markovian jump neural networks with time-varying delay via delay-product-type functionals. *IEEE Trans. Neural Netw. Learn. Syst.* **30**(8), 2528–2537 (2019)
- Song, Q., Chen, Y., Zhao, Z., Liu, Y., Alsaadi, F.E.: Robust stability of fractional-order quaternion-valued neural networks with neutral delays and parameter uncertainties. *Neurocomputing* **420**, 70–81 (2021)
- Dong, S., Zhu, H., Zhong, S., Shi, K., Cheng, J., Kang, W.: New result on reliable  $H_\infty$  performance state estimation for memory static neural networks with stochastic sampled-data communication. *Appl. Math. Comput.* **364**, 124619 (2020)
- Li, X., Nguang, S.K., She, K., Cheng, J., Shi, K., Zhong, S.: Stochastic exponential synchronization for delayed neural networks with semi-markovian switchings: saturated heterogeneous sampling communication. *Nonlin. Anal. Hybrid Syst.* **41**, 101028 (2021)
- Dong, S., Zhu, H., Zhang, Y., Zhong, S., Cheng, J., Shi, K.: Design of  $H_\infty$  state estimator for delayed static neural networks under hybrid-triggered control and imperfect measurement strategy. *J. Frankl. Inst.* **357**(17), 13231–13257 (2020)
- Shi, K., Wang, J., Tang, Y., Zhong, S.: Reliable asynchronous sampled-data filtering of T-S fuzzy uncertain delayed neural networks with stochastic switched topologies. *Fuzzy Sets Syst.* **381**, 1–25 (2020)
- Hua, L., Zhu, H., Shi, K., Zhong, S., Tang, Y., Liu, Y.: Novel finite-time reliable control design for memristor-based inertial neural networks with mixed time-varying delays. *IEEE Trans. Circuits Syst. I, Reg. Papers* **68**(4), 1599–1609 (2021)
- Ding, K., Zhu, Q.:  $H_\infty$  synchronization of uncertain stochastic time-varying delay systems with exogenous disturbance via intermittent control. *Chaos Solitons Fract.* **127**, 244–256 (2019)
- Wang, J., Ru, T., Xia, J., Shen, H., Sreeram, V.: Asynchronous event-triggered sliding mode control for semi-markov jump systems within a finite-time interval. *IEEE Trans. Circuits Syst. I, Reg. Papers* **68**(1), 458–468 (2021)
- Fan, X., Wang, Z.: Event-triggered sliding mode control for singular systems with disturbance. *Nonlin. Anal. Hybrid Syst.* **40**, 101011 (2021)
- Huang, J.: Adaptive fuzzy state/output feedback control of nonstrict-feedback systems: a direct compensation approach. *IEEE Trans. Cybern.* **49**(6), 2046–2059 (2019)
- Ding, D., Wang, Z., Han, Q.: Neural-network-based output-feedback control with stochastic communication protocols. *Automatica* **106**, 221–229 (2019)
- Mao, J., Ahn, C.K., Xiang, Z.: Global stabilization for a class of switched nonlinear time-delay systems via sampled-data output-feedback control. *IEEE Trans. Syst. Man Cybern. Syst.* (2021). <https://doi.org/10.1109/TSMC.2020.3048064>

22. Lu, J., Ho, D.W., Cao, J.: A unified synchronization criterion for impulsive dynamical networks. *Automatica* **46**(7), 1215–1221 (2010)
23. Li, X., Li, P.: Input-to-state stability of nonlinear systems: event-triggered impulsive control. *IEEE Trans. Autom. Control* (2021). <https://doi.org/10.1109/TAC.2021.3063227>
24. Liu, X., Zhang, K., Xie, W.: Pinning impulsive synchronization of reaction-diffusion neural networks with time-varying delays. *IEEE Trans. Neural Netw. Learn. Syst.* **28**(5), 1055–1067 (2017)
25. Lu, J., Kurths, J., Cao, J., Mahdavi, N., Huang, C.: Synchronization control for nonlinear stochastic dynamical networks: pinning impulsive strategy. *IEEE Trans. Neural Netw. Learn. Syst.* **23**(2), 285–292 (2012)
26. Li, S., Ahn, C.K., Chadli, M., Xiang, Z.: Sampled-data adaptive fuzzy control of switched large-scale nonlinear delay systems. *IEEE Trans. Fuzzy Syst.* (2021). <https://doi.org/10.1109/TFUZZ.2021.3052094>
27. Li, S., Ahn, C.K., Xiang, Z.: Sampled-data adaptive output feedback fuzzy stabilization for switched nonlinear systems with asynchronous switching. *IEEE Trans. Fuzzy Syst.* **27**(1), 200–205 (2019)
28. Fridman, E.: A refined input delay approach to sampled-data control. *Automatica* **46**(2), 421–427 (2010)
29. Ding, K., Zhu, Q.: A note on sampled-data synchronization of memristor networks subject to actuator failures and two different activations. *IEEE Trans. Circuits Syst. II, Exp. Briefs* **68**(6), 2097–2101 (2021)
30. Ni, X., Wen, S., Wang, H., Guo, Z., Zhu, S., Huang, T.: Observer-based quasi-synchronization of delayed dynamical networks with parameter mismatch under impulsive effect. *IEEE Trans. Neural Netw. Learn. Syst.* **32**(7), 3046–3055 (2021)
31. Li, X., Shen, J., Rakkiyappan, R.: Persistent impulsive effects on stability of functional differential equations with finite or infinite delay. *Appl. Math. Comput.* **329**, 14–22 (2018)
32. Wang, Y., Lu, J., Li, X., Liang, J.: Synchronization of coupled neural networks under mixed impulsive effects: a novel delay inequality approach. *Neural Netw.* **127**, 38–46 (2020)
33. Zhang, Q., Lu, J.: Impulsively control complex networks with different dynamical nodes to its trivial equilibrium. *Comput. Math. Appl.* **57**(7), 1073–1079 (2009)
34. Xie, X., Liu, X., Xu, H.: Synchronization of delayed coupled switched neural networks: mode-dependent average impulsive interval. *Neurocomputing* **365**, 261–272 (2019)
35. Jiang, B., Lu, J., Lou, J., Qiu, J.: Synchronization in an array of coupled neural networks with delayed impulses: average impulsive delay method. *Neural Netw.* **121**, 452–460 (2020)
36. Yao, F., Cao, J., Qiu, L., Cheng, P.: Input-to-state stability analysis of impulsive stochastic neural networks based on average impulsive interval. In: 2015 34th Chinese Control Conference (CCC), pp. 1775–1780 (2015)
37. Han, Y., Li, C., Zeng, Z.: Asynchronous event-based sampling data for impulsive protocol on consensus of non-linear multi-agent systems. *Neural Netw.* **115**, 90–99 (2019)
38. Seuret, A.: A novel stability analysis of linear systems under asynchronous samplings. *Automatica* **48**(1), 177–182 (2012)
39. Zeng, H., Teo, K., He, Y.: A new looped-functional for stability analysis of sampled-data systems. *Automatica* **82**, 328–331 (2017)
40. Zeng, H., Teo, K.L., He, Y., Wang, W.: Sampled-data stabilization of chaotic systems based on a T-S fuzzy model. *Inf. Sci.* **483**, 262–272 (2019)
41. Briat, C., Seuret, A.: A looped-functional approach for robust stability analysis of linear impulsive systems. *Syst. Control. Lett.* **61**(10), 980–988 (2012)
42. Shao, H., Zhao, J.: Dwell-time-dependent stability results for impulsive systems. *IET Control. Theory Appl.* **11**(7), 1034–1040 (2017)
43. Briat, C., Seuret, A.: Stability criteria for asynchronous sampled-data systems—a fragmentation approach. *IFAC Proc. Volumes* **44**(1), 1313–1318 (2011)
44. Li, P., Liu, X., Zhao, W., Zhong, S.: A new looped-functional for stability analysis of the linear impulsive system. *Commun. Nonlinear Sci. Numer. Simul.* **83**, 105140 (2020)
45. Fan, Y., Huang, X., Shen, H., Cao, J.: Switching event-triggered control for global stabilization of delayed memristive neural networks: an exponential attenuation scheme. *Neural Netw.* **117**, 216–224 (2019)
46. Wang, X., Wang, Z., Song, Q., Shen, H., Huang, X.: A waiting-time-based event-triggered scheme for stabilization of complex-valued neural networks. *Neural Netw.* **121**, 329–338 (2020)
47. Liu, Y., Wang, Z., Liu, X.: Global exponential stability of generalized recurrent neural networks with discrete and distributed delays. *Neural Netw.* **19**(5), 667–675 (2006)
48. Friedman, A.: Stochastic differential equations and applications. In: *Stochastic Differential Equations*, pp. 75–148 (2010)
49. Yi, C., Feng, J., Wang, J., Xu, C., Zhao, Y.: Synchronization of delayed neural networks with hybrid coupling via partial mixed pinning impulsive control. *Appl. Math. Comput.* **312**, 78–90 (2017)

**Publisher's Note** Springer Nature remains neutral with regard to jurisdictional claims in published maps and institutional affiliations.